Measuring FORCs diagrams in computer simulations as a mean to gain microscopic insight

Dobroserdova, A. B.; Sanchez Romero, P. A.; Shapochkin, V. E.; Smagin, D. A.; Zverev, V. S.; Odenbach, S.; Kantorovich, S. S.;

Originally published:

May 2020

Journal of Magnetism and Magnetic Materials 501(2020), 166393

DOI: https://doi.org/10.1016/j.jmmm.2020.166393

Perma-Link to Publication Repository of HZDR:

https://www.hzdr.de/publications/Publ-31292

Measuring FORCs diagrams in computer simulations as a mean to gain microscopic insight

Dobroserdova A.B.[a], Sánchez P.A.[a,b], Shapochkin V.E.[a], Smagin D.A.[a], Zverev V.S.[a], Odenbach S.[c], Kantorovich S.S.[a,d]

[a] *Ural Federal University, Lenin Av. 51, Ekaterinburg, Russia*
[b] *Helmholtz-Zentrum Dresden-Rosendorf, Bautzner Landstrasse 400, Dresden, Germany*
[c] *Technological University of Dresden, George-Bähr-Strasse 3, Dresden, Germany*
[d] *University of Vienna, Sensengasse 8, Vienna, Austria*

Abstract

FORCs (first-order reversal curves) diagrams prove to be an efficient experimental technique to investigate magnetic interactions in complex systems. In experiments, as a rule, it is difficult to relate actual microstructural changes to the evolution of FORCs diagrams. Here, using Molecular Dynamics simulations, we calculate FORCs for two simple models of a magnetic elastomer. The simplicity of these models allows to relate directly both, the rigidity of the matrix and the magnetoelastic coupling to the shape and intensity of FORCs diagrams.

Keywords: FORC, Molecular Dynamics, magnetic elastomers, magneto-elastic coupling

1. Introduction

Magnetic elastomers are systems consisting of magnetic particles embedded in a non-magnetic elastic matrix. Such systems have a wide range of applications, from technical devices as magnetically controlled actuators and damping systems to artificial muscles and soft robotics [1].

Diagrams of first-order reversal curves (FORCs) are a sensitive tool to characterise magnetic hysteretic behaviour [2, 3]. FORCs diagrams have an advantage over well-known ΔM-experimental procedures, as they do not require to measure magnetisation in a remanent state and allow to avoid AC measurements in demagnetised state [4]. Pike and coauthors used FORCs diagrams to investigate various magnetic-particle-based systems [5, 6, 7, 8].

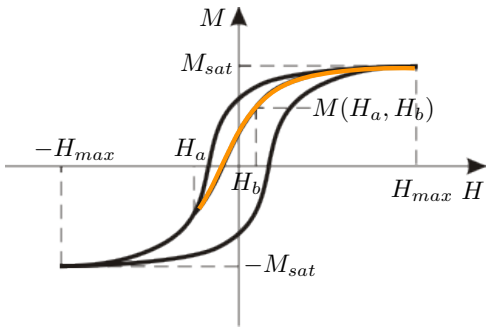

Figure 1: Sketch of a typical hysteresis curve with the first order reversal curve (in orange).

In general, a FORCs diagram is calculated in the following way. First, the hysteresis loop of a system of interest is measured. Next, a set of partial hysteresis curves, or FORCs [9], is obtained. In Fig. 1 we show a scheme of FORCs calculations. Initially, the sample is saturated to M_{sat}, by magnetising it at field H_{max}. Once the hysteresis loop between $[-H_{max}, H_{max}]$ is obtained (black), the field is decreased to a reversal field H_a. The FORC is the curve (plotted in orange in Fig. 1) that shows the magnetisation path from H_a back to saturation. This procedure is repeated for many different values of $H_a \leqslant H_b$. From all these FORCs, one can construct a two-dimensional function $M(H_a, H_b)$. The FORCs distribution, by definition, is the mixed second derivative:

$$\rho(H_a, H_b) = -\frac{\partial^2 M(H_a, H_b)}{\partial H_a \partial H_b}. \quad (1)$$

Conventionally, in order to plot a FORCs diagram, one changes the coordinates from $\{H_a, H_b\}$ to $\{H_c = (H_b - H_a)/2, H_u = (H_a + H_b)/2\}$, where H_c denotes the coercive field, whereas H_u is usually addressed as a local interaction field. The outcome is a contour plot in the positive H_c half-plane.

Recently, FORCs measurements were successfully applied to characterise hybrid elastomers [10, 11]. Inspired by these works, as well as by the efficiency of coarse-grained computer models of such materials applied to elucidate the relationship between their microstructural changes and magnetic response [12], we decided to employ the same simulation approaches to model the relationship between FORCs diagrams and microscopic properties. The two computer models introduced in Reference [12] use an implicit representation of the polymer matrix in the form of elastic constraints acting on the movement of explicit magnetic particles. In the first model, only translational motion of the particles is restricted, whereas in the second one both, translations and rotations are penalised. Here, we

Email address: Alla.Dobroserdova@urfu.ru (Dobroserdova A.B.)

study the effect of the matrix rigidity on FORCs for both models, varying additionally the interparticle interaction strength.

2. Simulation Approach

2.1. General Scheme

We have performed Molecular Dynamics simulations [13] with the software package ESPResSo 3.3.1 [14, 15]. We used a Langevin thermostat under quasi-athermal and periodic boundary conditions. We considered only magnetoactive elastomers filled with monodisperse magnetically hard particles, that we model as identical ideal spheres having a characteristic diameter σ and a point magnetic dipole $\vec{m}$ located at their centres. Therefore, the main interaction between them is described by the magnetic dipole-dipole potential [16], that in dimensionless units can be written as:

$$U_{\mathrm{dd}}(i,j) = \left(\frac{\langle \vec{m}_i, \vec{m}_j \rangle}{|\vec{r}_{ij}|^3} - \frac{3}{|\vec{r}_{ij}|^5} \langle \vec{m}_i, \vec{r}_{ij} \rangle \langle \vec{m}_j, \vec{r}_{ij} \rangle \right), \quad (2)$$

where $\vec{m}_i$ and $\vec{m}_j$ are magnetic moments of i^{th} and j^{th} particles, respectively, and $\vec{r}_{ij}$ is the vector connecting their centres.

The steric repulsion between magnetic particles is described by a truncated and shifted Lennard-Jones potential, also known as the Weeks-Chandler-Andersen (WCA) potential [17]:

$$U_{\mathrm{WCA}}(i,j) = \begin{cases} 4\left[\left(\frac{\sigma}{|\vec{r}_{ij}|} \right)^{12} - \left(\frac{\sigma}{|\vec{r}_{ij}|} \right)^{6} \right] + c_{\mathrm{shift}}, & |\vec{r}_{ij}| \le r_{\mathrm{cut}}, \\ 0, & |\vec{r}_{ij}| > r_{\mathrm{cut}}, \end{cases} \quad (3)$$

where $r_{\mathrm{cut}} = 2^{1/6}\sigma$ is the truncation distance that makes the potential purely repulsive and c_{shift} is the value of the Lennard-Jones term at $|\vec{r}_{ij}| = r_{\mathrm{cut}}$.

The Zeeman potential describes the interaction between magnetic particles with point dipoles and any uniform applied magnetic field, $\vec{H}$:

$$U_{\mathrm{H}}(i) = -\langle \vec{m}_i, \vec{H} \rangle. \quad (4)$$

In order to model the polymer matrix as elastic constraints we use classical harmonic springs connecting the magnetic particles and randomly distributed fixed points in space:

$$U_{\mathrm{K}}(r) = \frac{K}{2} r^2. \quad (5)$$

where r is the elongation of the spring and K its elastic constant, that represents the rigidity of the matrix. In all cases the values of K have been taken from a normal distribution ranging a given interval.

2.2. Penalty on particle translation. Model M1

The simplest model (M1) only considers translational constraints on the magnetic particles. This is achieved by attaching one end of a single spring to the centre of each particle, as shown in Fig. 2(a). The other end is fixed to an anchoring point that corresponds to the elastic equilibrium position of the particle.

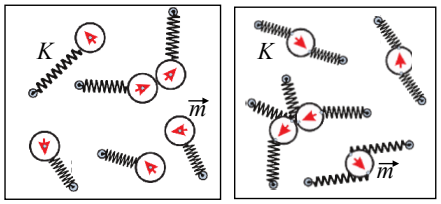

(a) (b)

Figure 2: (a) Model M1: each magnetic particle centre is connected to one end of a harmonic spring, whose other end is attached to a fixed anchoring point. (b) Model M2: two springs are attached to the surface of each magnetic particle, at the points corresponding to the projections of the head and the tail of the central dipole. Each spring is also attached to a different anchoring point. Springs rigidity constant is K, particle magnetic moment is $\vec{m}$.

2.3. Penalty on particle translation and rotation. Model M2

In the second case (M2) both, translations and rotations of the particles are elastically constrained. This is achieved for each particle by attaching two identical harmonic springs that connect two different anchoring points and the surface of the particle at the projection points of the head and the tail of its central dipole, as shown in Fig. 2(b). Therefore, the elastic equilibrium position of each particle corresponds to a perfect alignment of its dipole with the anchoring points.

2.4. The nature of the hysteresis in the model

We perform molecular dynamics simulations at very low temperature. So, at each field value H, there's a local minimum of the system energy, corresponding to optimised dipolar, Zeeman and elastic forces. The system is trapped in this minimum and any attempt to increase or decrease the magnetic field will move the system away from the given state after the barrier is overcome. So, on the simulation timescale, it does not matter how many times we integrate the system at a given field, as long as the number of steps is sufficient for the system to reach the local minima. To illustrate the character of the magnetic hysteresis, in Fig. 3, we plot several loops obtained with different amount of integrations as indicated in the legend. It can clearly be seen, that the loop is stable.

—

3. Results and Discussions

3.1. The impact of matrix rigidity and dipolar interactions on FORCs in M1

In Fig. 4 we plot eight FORCs diagrams for M1 model elastomers with different dimensionless values of matrix rigidity and magnetic moment of the particles. In the upper row, corresponding to $|\vec{m}| = 1.0$, the point of maximum intensity of the diagrams stays at zero independently from matrix rigidity, that grows from left to right. By increasing the mean value of K by factor of almost five (compare Fig. 4(a) and 4(d)), one can notice only a slight shortening of the bright region along H_c axis. The situation drastically changes if the interparticle interaction strength grows, as shown in the lower row, where $|\vec{m}| = 2.0$.

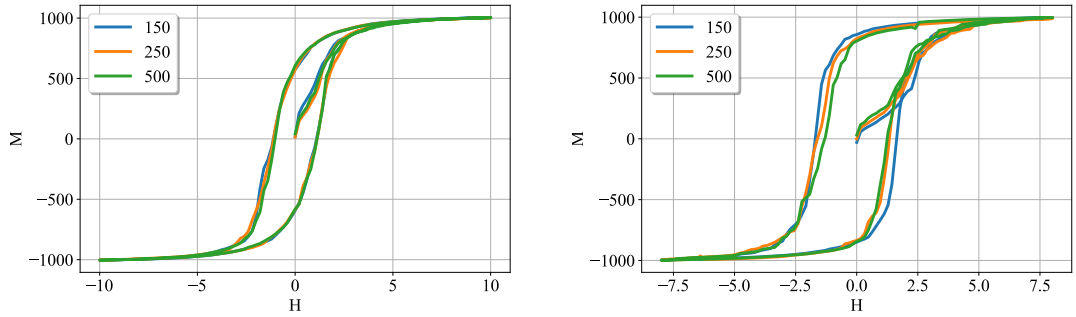

Figure 3: Hysteresis loops with different numbers of integrations performed at each value of H. The number of integrations are given in the legends. (a): model M1, $K \in [30, 40]$, $|\vec{m}| = 2.0$. (b): model M2, $K \in [0.5, 1.0]$, $|\vec{m}| = 2.0$.

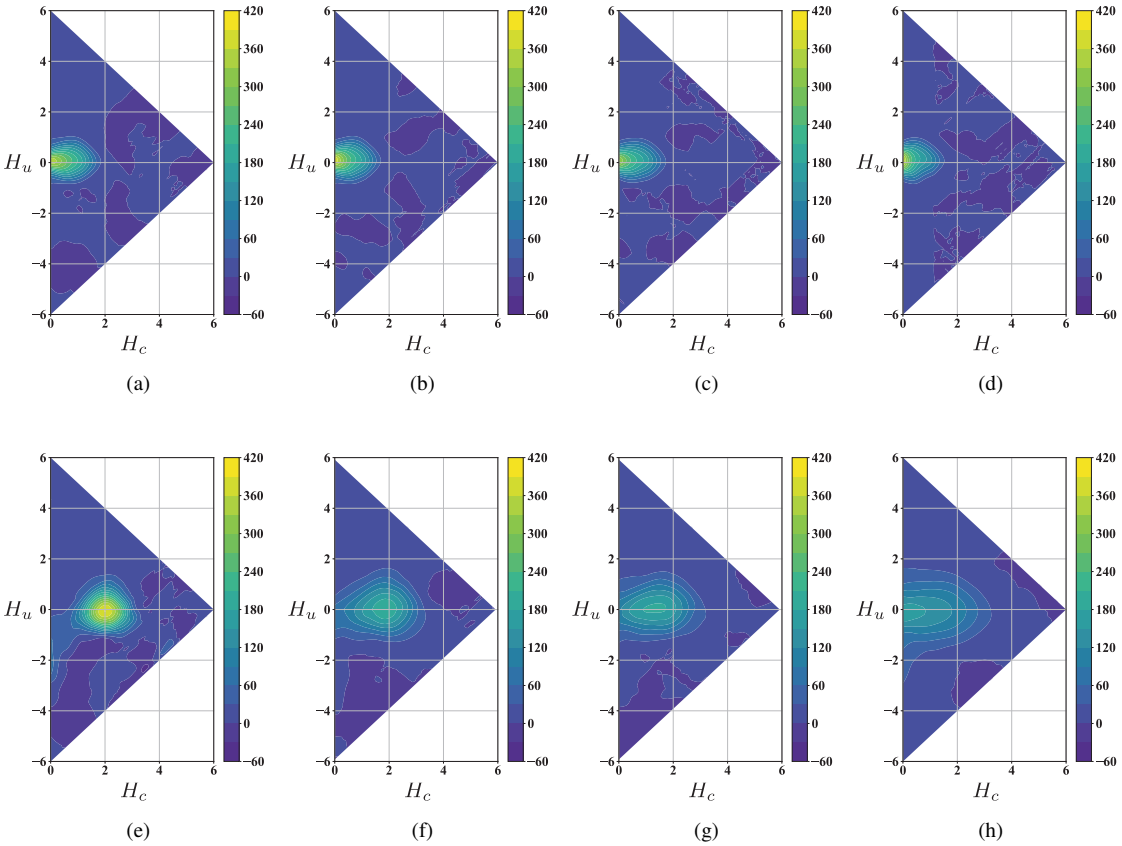

Figure 4: FORCs diagrams for M1. Particle magnetic moment is constant in each row: (a)–(d) $|\vec{m}| = 1.0$; (e)–(h) $|\vec{m}| = 2.0$; The rigidity constant K is the same in each column: (a) and (e) $K \in [5, 10]$; (b) and (f) $K \in [10, 20]$; (c) and (g) $K \in [20, 30]$; (d) and (h) $K \in [30, 40]$.

First of all the maximum of the intensity shifts to nonzero values of H_c. This shift is especially pronounced for the soft matrix, see Fig. 4(e). For this system the intensity is also the highest and the region of the maximum is highly localised. With increasing rigidity, the coercive field corresponding to the point of maximal intensity shifts to the left (compare, for example, Fig. 4(f) and 4(h)). Moreover, the overall shape of the high-value region is changing, from a circular to an elongated shape. It is worth mentioning that in case of M1, when only translation of magnetic particles is penalised by springs, FORCs are symmetric with respect to local interaction field H_u.

Summarising this part, we find that the increase of interparticle interactions in an elastomer with rotationally non-constrained magnetic particles leads to the shift of the FORCs diagram maximum towards larger values of H_c and broader distribution along H_u. The effect of growing matrix rigidity is also reflected in FORCs through the opposite shift in values of H_c; moreover, the maximum becomes less pronounced.

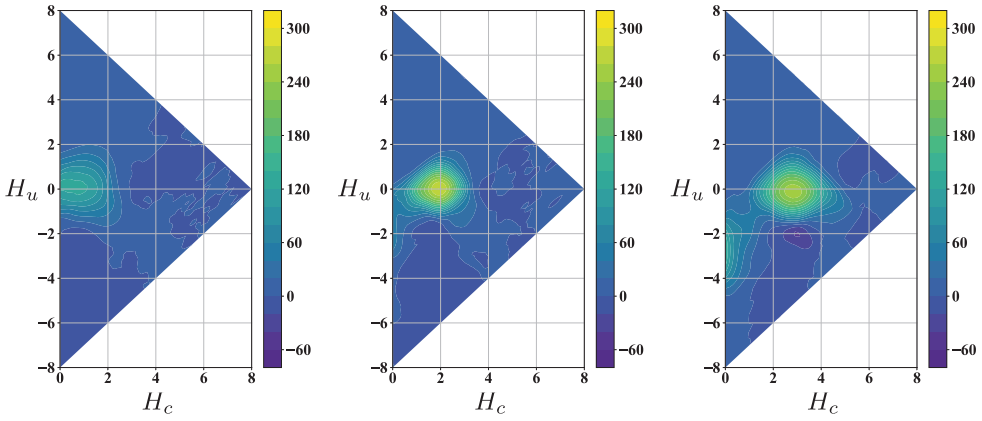

Figure 5: FORCs diagrams for M2, $K \in [0.5, 1.0]$. (a) $|\vec{m}| = 1.41 \approx \sqrt{2}$; (b) $|\vec{m}| = 2.0 = \sqrt{4}$; (c) $|\vec{m}| = 2.45 \approx \sqrt{6}$.

3.2. The impact of magnetoelastic coupling and dipolar strength. Model M2

Constraining both, rotations and translations of magnetic particles leads to qualitative changes in FORCs diagrams, as evidenced by Fig. 5. Here, we plot FORCs diagrams for M2 model elastomers corresponding to three different strengths of the magnetic moments of their particles, that grow from left to right. For weak dipole moments, FORCs diagram in Fig. 5(a) looks qualitatively similar to its corresponding counterpart in M1 systems (see Fig. 4(a)). However, in this case the spread along H_u is larger. As in M1 systems, with growing dipole strength the maximum of the FORCs diagram shifts to the right (compare, for example, Fig. 5(b) and Fig. 5(c)). The qualitative difference between FORCs diagrams corresponding to M1 and M2 systems is that in the second case the symmetry along the H_u axis tends to be lost. This is especially clear in Fig. 5(c).

In summary, the analysis of M2 elastomer FORCs diagrams reveals that asymmetries of the high intensity region can stem from the constraints on rotational degrees of freedom of the magnetic particles. This effect is particularly pronounced when magnetic interparticle interactions are sufficiently strong.

4. Conclusions

In this work we presented in-silico analysis of FORCs diagrams for two simple coarse-grained models of magnetic elastomers. In the first model the elastic matrix, modelled by harmonic springs, hinders only translational motion of magnetic particles. Thus, if an external magnetic field is applied, particles can freely reorient, but their self-assembly is hindered. In the second model, not only translation, but also reorientation of magnetic particles is penalised. This way, the matrix hinders not only the self-assembly driven by interparticle magnetic forces, but also the overall magnetisation of the sample. In both models only elastic deformations were considered. We analysed the influence of both dipolar strength and matrix rigidity on the shape and intensity of FORCs diagrams. We found that, independently from model and matrix rigidity, the increase of dipolar strength, responsible for interparticle correlations and self-assembly, results in the shift of the maximum of intensity of the FORCs diagram towards higher values of the coercive field. Moreover, if only particle translational degrees of freedom are coupled to the matrix and the interparticle interaction is sufficiently strong, the growth of springs rigidity results in the shift of the maximum of FORCs diagram towards smaller values of coercive field and is accompanied by a broadening of the high intensity region in the vertical direction. Finally, in elastomers where only particle translations are hindered by the elastic matrix, we observed no asymmetry of FORCs diagrams with respect to horizontal direction, i.e. the values of FORCs diagrams are the same if the local interaction field is inverted. Such an asymmetry, however, is observed for the second model, and it is enhanced with the strengthening of the dipole moments. Strong dipole-dipole interparticle interactions lead to a more pronounced self-assembly and, thus, the local minima of the energy landscape get deeper, that manifests itself the FORC diagrams. Although we do not aim at quantitative descriptions of real elastomers, the effects found here are expected to be observed in magnetic elastomers with magnetically hard particles, like NeFeB, and various constraints reflect the coupling between particle surface and polymer matrix

5. Acknowledgements

This research has been supported by the RFBR-DFG Grant 19-52-12028, Act 211 Government of the Russian Federation, Contract 02.A03.21.0006, the Ministry of Education and Science of the Russian Federation, Project 3.1438.2017/4.6. S.S.K. acknowledges support from the Austrian Research Fund (FWF), START-Projekt Y 627-N27. S.Od. acknowledges support from the DFG Od 18/24-1 within SPP1681 and PAK907.

References

[1] W. H. Li, X. Z. Zhang, H. Du., Magnetorheological elastomers and their applications, Advances in Elastomers 11 (2013) 357–374.

[2] F. Preisach, Über die magnetische nachwirkung, Zeitschrift für Physik 94 (5) (1935) 277–302. doi:10.1007/BF01349418.

[3] C. R. Pike, A. P. Roberts, M. J. Dekkers, K. L. Verosub, An investigation of multi-domain hysteresis mechanisms using forc diagrams, Physics of the Earth and Planetary Interiors 126 (1) (2001) 11 – 25, rock Magnetism Enters the New Millenium. A Celebration of Fifty Years of Neel's Theories. doi:https://doi.org/10.1016/S0031-9201(01)00241-2.

[4] A. Stancu, C. Pike, L. Stoleriu, P. Postolache, D. Cimpoesu, Micromagnetic and preisach analysis of the first order reversal curves (forc) diagram, Journal of Applied Physics 93 (10) (2003) 6620–6622. doi:10.1063/1.1557656.

[5] C. Pike, A. Fernandez, An investigation of magnetic reversal in submicron-scale co dots using first order reversal curve diagrams, Journal of Applied Physics 85 (9) (1999) 6668–6676. doi:10.1063/1.370177.

[6] C. Pike, A. Roberts, K. Verosub, Characterizing interactions in fine magnetic particle systems using first order reversal curves, Journal of Applied Physics 85 (9) (1999) 6660–6667. doi:10.1063/1.370176.

[7] C. R. Pike, A. P. Roberts, K. L. Verosub, First order reversal curve diagrams and thermal relaxation effects in magnetic particles, Geophysical Journal International 145 (3) (2001) 721–730. doi:10.1046/j.0956-540x.2001.01419.x.

[8] A. P. Roberts, C. R. Pike, K. L. Verosub, First-order reversal curve diagrams: A new tool for characterizing the magnetic properties of natural samples, Journal of Geophysical Research: Solid Earth 105 (B12) (2000) 28461–28475. doi:10.1029/2000JB900326.

[9] I. Mayergoyz, Mathematical models of hysteresis, IEEE Transactions on Magnetics 22 (5) (1986) 603–608. doi:10.1109/TMAG.1986.1064347.

[10] J. Linke, D. Y. Borin, S. Odenbach, First-order reversal curve analysis of magnetoactive elastomers, RSC Adv. 6 (2016) 100407–100416. doi:10.1039/C6RA23435F.

[11] M. Vaganov, J. Linke, S. Odenbach, Y. Raikher, Model forc diagrams for hybrid magnetic elastomers, Journal of Magnetism and Magnetic Materials 431 (2017) 130–133. doi:10.1016/j.jmmm.2016.08.084.

[12] P. A. Sánchez, T. Gundermann, A. B. Dobroserdova, S. S. Kantorovich, S. Odenbach, Importance of matrix inelastic deformations in the initial response of magnetic elastomers, Soft Matter 14 (2018) 2170–2183. doi:10.1039/c7sm02366a.

[13] M. P. Allen, D. J. Tildesley, Computer Simulation of Liquids, 1st Edition, Oxford Science Publications, Clarendon Press, Oxford, 1987.

[14] H. J. Limbach, A. Arnold, B. A. Mann, C. Holm, ESPResSo – an extensible simulation package for research on soft matter systems, Computer Physics Communications 174 (9) (2006) 704–727. doi:10.1016/j.cpc.2005.10.005.

[15] J. J. Cerdà, V. Ballenegger, O. Lenz, C. Holm, P3m algorithm for dipolar interactions, Journal of Chemical Physics 129 (2008) 234104. doi:10.1063/1.3000389.

[16] E. M. Purcell, Electricity and Magnetism, Berkeley Physics Course, Vol. 2, McGraw-Hill Science/Engineering/Math, 1984.

[17] J. D. Weeks, D. Chandler, H. C. Andersen, Role of repulsive forces in determining the equilibrium structure of simple liquids, Journal of Chemical Physics 54 (1971) 5237–5247.